# Articles

## Mechanistic Details for the Electroreduction of Fluorophenyl σ-Bonded Iron(III) Porphyrins in Noncoordinating Solvents

**Karl M. Kadish,*[1a] Francis D'Souza,[1a] Eric Van Caemelbecke,[1a] Anne Villard,[1a] Jae-Duck Lee,[1a,b] Alain Tabard,[1c] and Roger Guilard*[1c]**

Department of Chemistry, University of Houston, Houston, Texas 77204-5641, and Laboratoire d'Ingénièrie Moléculaire pour la Séparation et les Applications des Gaz Associé au CNRS (LIMSAG), UMR 9953, Faculté des Sciences "Gabriel", Université de Bourgogne, 6 Boulevard Gabriel, 21100 Dijon, France

*Received April 2, 1993*®

A self-consistent mechanism for the reduction of fluorophenyl σ-bonded iron(III) porphyrins in noncoordinating solvents was elucidated using electrochemical and spectroelectrochemical techniques. The investigated porphyrins are represented as (P)Fe($C_6F_5$) and (P)Fe($C_6F_4H$) where P is the dianion of octaethylporphyrin (OEP), tetraphenylporphyrin (TPP), tetra-*m*-tolylporphyrin (TmTP), tetra-*p*-tolylporphyrin (TpTP), or tetrakis(*p*-(trifluoromethyl)phenyl)porphyrin (Tp-$CF_3$PP). Each σ-bonded compound undergoes up to seven different redox processes, some of which are associated with the initial σ-bonded complex while others are associated with the products of the initial or following electron-transfer reactions. The mechanism for reduction of (P)Fe($C_6F_5$) and (P)Fe($C_6F_4H$) differs from that of all previously investigated iron porphyrins, and this is due entirely to the presence of the σ-bonded fluorophenyl ligand. The first reduction of (P)Fe(R) leads to (P)$Fe^{II}$ and $R^-$, the latter of which reacts with trace water in solution to give $OH^-$ and RH. The generated $OH^-$ displaces the axial fluorophenyl ligand from unreduced (P)Fe(R), and this sets in motion a chain reaction which continues until all of the σ-bonded porphyrin is converted to monomeric (P)FeOH prior to formation of dimeric $[(P)Fe]_2O$ on longer time scales. The same Fe(III) porphyrin products can also be obtained by addition of substoichiometric amounts of $F^-$ or $OCH_3^-$ to (P)Fe(R), and this occurs because both anions are able to displace the fluorophenyl axial ligand from (P)Fe(R) and initiate the chain reaction in the absence of any electrochemistry.

### Introduction

Iron(III) porphyrins containing σ-bonded $C_6F_5$ or $C_6F_4H$ axial ligands were first characterized in benzonitrile[2] and later in more detail in pyridine[3] where relatively stable six-coordinate complexes are formed. These derivatives can be reversibly reduced to the Fe(II) σ-bonded complex in pyridine, but this is not the case in noncoordinating solvents where the addition of one electron to the metal center is followed by a rapid cleavage of the iron–carbon bond and the apparent formation of the (P)$Fe^{II}$ complex where P is the dianion of a given porphyrin macrocycle.[2] The basis of this assignment was the presence of an irreversible one-electron reduction which was followed by a second reversible one-electron reduction at potentials corresponding to the (P)$Fe^{II}$/$[(P)Fe^{I}]^-$ potentials of the non-σ-bonded complex.

The number of reversible processes for a given iron(III) porphyrin will depend upon the nature of the axial and equatorial (macrocyclic) ligand as well as upon the solvent.[4-6] Almost all complexes with anionic axial ligands can undergo up to three one-electron reductions in nonaqueous media, and these correspond to the stepwise formation of Fe(II) derivatives, Fe(I) derivatives, and Fe(I) porphyrin π anion radicals. In contrast, only one or two one-electron reductions are seen for σ-bonded derivatives of the type (P)Fe(R) where R represents $C_6H_5$, $C_6F_5$, or $C_6F_4H$.[2,7,8]

The reduction of phenyl- and (fluorophenyl)iron porphyrins and the resulting cyclic voltammograms initially appeared to be straightforward,[2,3] but more detailed studies utilizing a variety of macrocycles with different basicities now indicate that not all of the observed redox processes of (P)Fe($C_6F_5$) and (P)Fe($C_6F_4H$) can be accounted for by a simple ligand dissociation reaction following the initial electron-transfer step. This is discussed in the present paper which provides new data on the electrochemistry and spectroelectrochemistry of penta- and tetrafluorophenyl σ-bonded iron(III) porphyrin derivatives and elucidates the nature of the coupled chemical reactions which occur in benzonitrile and methylene chloride. The investigated porphyrins are represented as (P)Fe($C_6F_5$) and (P)Fe($C_6F_4H$) where P is the dianion of octaethylporphyrin (OEP), tetraphenylporphyrin (TPP), tetra-*m*-tolylporphyrin (TmTP), tetra-*p*-tolylporphyrin (TpTP), or tetrakis(*p*-(trifluoromethyl)phenyl)porphyrin (Tp-$CF_3$PP).

### Experimental Section

**Chemicals.** Synthesis and handling of the (σ-aryl)iron porphyrins was carried out under an argon atmosphere. All common solvents were purified in an appropriate manner[9] and were distilled under argon prior to use. Methylene chloride ($CH_2Cl_2$) for the electrochemical studies was distilled

• Abstract published in *Advance ACS Abstracts,* August 15, 1993.

(1) (a) University of Houston. (b) On leave from Dong-A University, Korea. (c) University of Burgundy.
(2) Guilard, R.; Boisselier-Cocolios, B.; Tabard, A.; Cocolios, P.; Simonet, B.; Kadish, K. M. *Inorg. Chem.* **1985**, *24*, 2509–2520.
(3) Kadish, K. M.; Tabard, A.; Lee, W.; Liu, Y. H.; Ratti, C.; Guilard, R. *Inorg. Chem.* **1991**, *30*, 1542–1549.
(4) Kadish, K. M. *Prog. Inorg. Chem.* **1986**, *34*, 435–605.
(5) Guilard, R.; Kadish, K. M. *Chem. Rev.* **1988**, *88*, 1121–1146.
(6) Guilard, R.; Lecomte, C.; Kadish, K. M. *Struct. Bonding* **1987**, *64*, 205–268.
(7) Lançon, D.; Cocolios, P.; Guilard, R.; Kadish, K. M. *J. Am. Chem. Soc.* **1984**, *106*, 4472–4478.
(8) Lançon, D.; Cocolios, P.; Guilard, R.; Kadish, K. M. *Organometallics* **1984**, *3*, 1164–1170.
(9) Perrin, D. D.; Armarego, W. L. F.; Perrin, D. R. *Purification of Laboratory Chemicals*, 2nd ed.; Pergamon Press: New York, 1980.

0020-1669/93/1332-4179$04.00/0 © 1993 American Chemical Society

over $CaH_2$ while benzonitrile (PhCN) was distilled over $P_2O_5$ under reduced pressure. Tetra-*n*-butylammonium hexafluorophosphate ((TBA)$PF_6$) was obtained from Alfa Chemicals and recrystallized from an ethyl acetate/hexane mixture prior to use. Tetra-*n*-butylammonium perchlorate (TBAP) from Eastman Chemicals was recrystallized from ethyl acetate and then dried in vacuo at 40 °C. Tetra-*n*-butylammonium fluoride ((TBA)F) was also obtained from Eastman Chemicals and was used as received. The $\sigma$-bonded arylporphyrins, (P)Fe($C_6H_5$) and (P)Fe($C_6F_4X$) where X = H or F, were prepared by the action of RMgBr (R = $C_6H_5$, $C_6F_5$, or $C_6F_4H$) on the respective porphyrin iron(III) chloride, (P)FeCl, as described in previous publications.[2,3] (Tetrakis(2,4,6-trimethylphenyl)-porphyrinato)iron(III) chloride and hydroxide, (TMP)FeCl and (TMP)-FeOH, were synthesized according to literature procedures.[10]

**Instrumentation.** Cyclic voltammetry was carried out with an EG&G Model 173 potentiostat, an IBM Instruments Model EC 225 voltammetric analyzer, or a BAS 100 electrochemical analyzer. Current–voltage curves were recorded on a Houston Instruments Model 2000 X-Y recorder or a Houston Instruments HIPLOT DMP-40 plotter. A three-electrode system was used and consisted of a platinum or a glassy carbon button working electrode, a platinum wire counter electrode, and a saturated calomel electrode (SCE) as reference. The reference electrode was separated from the bulk of the solution by a fritted-glass bridge filled with the solvent and supporting electrolyte. Solutions containing only the supporting electrolyte were deoxygenated by a stream of nitrogen for at least 10 min before introduction of the porphyrin and were protected from air by a nitrogen blanket during the experiment. Rotating disk electrode (RDE) voltammetry was performed with an MSR Speed Control Unit (Pine Instrument Co.). A platinum RDE of area 0.198 $cm^2$ was employed as the working electrode. All potentials are referenced to the SCE.

Spectroelectrochemical experiments and thin-layer coulometry were performed at a platinum thin-layer electrode.[11] Potentials were monitored with an IBM Instruments Model EC 225 voltammetric analyzer. Time-resolved UV–visible spectra were recorded with a Tracor Northern Model 6500 rapid-scan spectrophotometer/multichannel analyzer. Bulk controlled potential coulometry was carried out in an "H" cell using a three-electrode system in which a large platinum gauze electrode served as the working electrode.

## Results and Discussion

**Electroreduction of (Tp-$CF_3$PP)Fe($C_6H_5$), (Tp-$CF_3$PP)Fe($C_6F_4X$), and (Tp-$CF_3$PP)FeCl Where X = H or F.** Figure 1 shows cyclic voltammograms of (Tp-$CF_3$PP)Fe($C_6H_5$), (Tp-$CF_3$PP)Fe($C_6F_4X$), and (Tp-$CF_3$PP)FeCl in benzonitrile containing 0.1 M (TBA)$PF_6$. The $\sigma$-bonded phenyl derivative undergoes two reversible one-electron reductions at $E_{1/2}$ = –0.57 and –1.84 V. Both the singly- and doubly-reduced products are stable on the cyclic voltammetry time scale, and no cleavage of the $C_6H_5$ axial ligand is observed to occur. Two one-electron reductions have earlier been reported for ((CN)$_4$TPP)Fe($C_6H_5$) under the same solution conditions,[2] and to date, these two complexes are the only $\sigma$-bonded Fe(III) porphyrins to show this type of redox behavior. The difference in potential between the first and second reductions of (Tp-$CF_3$PP)Fe($C_6H_5$) is 1.27 V (see Figure 1a), and this value is larger than the $\Delta E_{1/2}$ of 0.99 V between the two one-electron reductions of ((CN)$_4$TPP)Fe($C_6H_5$).

The first one-electron reduction of (Tp-$CF_3$PP)Fe($C_6F_4H$) or (Tp-$CF_3$PP)Fe($C_6F_5$) is reversible at scan rates greater than 0.1 V/s when the potential is scanned between 0.00 and –0.50 V but not when scanning is extended to more negative potentials (Figure 1b). The initial reduction of (Tp-$CF_3$PP)Fe(R) (process I) occurs at $E_{1/2}$ = –0.34 V (R = $C_6F_5$) or –0.38 V (*R* = $C_6F_4H$) and is followed by four additional processes which are labeled as II–V. The difference in potentials between $E_{1/2}$ for process I of the two fluorophenyl $\sigma$-bonded metalloporphyrins is consistent with the different electron-withdrawing natures of the $C_6F_5$ and $C_6F_4H$ axial ligands, but no such trend in $E_{1/2}$ is observed for processes II–V which occur at similar potentials, independent of the axial ligand.

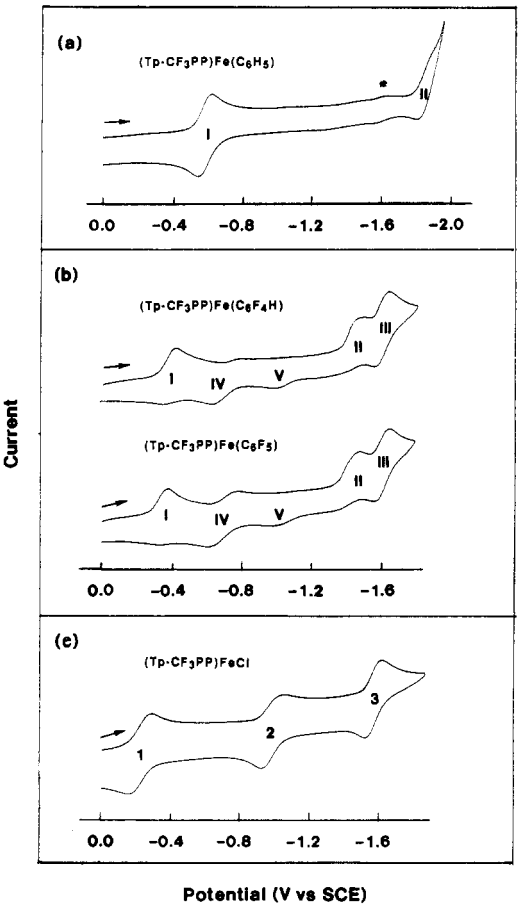


**Figure 1.** Cyclic voltammograms of (a) (Tp-$CF_3$PP)Fe($C_6H_5$), (b) (Tp-$CF_3$PP)Fe($C_6F_4H$) and (Tp-$CF_3$PP)Fe($C_6F_5$), and (c) (Tp-$CF_3$PP)FeCl in PhCN containing 0.2 M (TBA)$PF_6$. Scan rate = 0.1 V/s. The asterisk in part a indicates a solvent impurity.

The earlier proposed loss of a $C_6F_5$ or $C_6F_4H$ axial ligand from electroreduced (P)Fe($C_6F_4X$) was based in large part on the fact that $E_{1/2}$ for the second reduction of (P)FeCl, i.e. the Fe(II)/Fe(I) reaction, occurred at a potential identical with that for reduction of the chemical "decomposition" product of electroreduced (P)Fe($C_6F_4X$)[2] (which, in this paper, is labeled as process V). However, a close examination of the data in ref 2 for five different $Cl^-$ or $C_6F_4X$ derivatives (X = H or F) shows that these half-wave potentials may or may not be superimposable for a given series of Fe(III) porphyrins having the same macrocyclic ring but different axial ligands. This comparison is illustrated in Figure 1b,c for (Tp-$CF_3$PP)Fe complexes with $C_6F_4H$, $C_6F_5$, and $Cl^-$ axial ligands. The reduction of (Tp-$CF_3$PP)FeCl (Figure 1c) involves three reversible one-electron transfers, as is also the case for reduction of other (P)FeCl species in PhCN.[4,12] The second reduction of (Tp-$CF_3$PP)FeCl occurs at $E_{1/2}$ = –0.98 V in PhCN, and this value is identical to the $E_{1/2}$ for process V of (Tp-$CF_3$PP)Fe($C_6F_4X$) where X = H or F (see Table I). It is also similar to $E_{1/2}$ for the first one-electron reduction of the related $\mu$-oxo dimer, [(Tp-$CF_3$PP)Fe]$_2$O.[13] The half-wave potential for process 3 of (Tp-$CF_3$PP)FeCl (–1.60 V) is similar to $E_{1/2}$ for process III of (Tp-$CF_3$PP)Fe($C_6F_4X$) (see Table I), and this suggests the same reacting species in solution.

Figure 2 illustrates cyclic voltammograms of (Tp-$CF_3$PP)-Fe($C_6F_4H$) taken in PhCN under conditions of different switching potentials. The ratio of the anodic-to-cathodic peak currents for process I, $i_{pa}/i_{pc}$, is approximately 1.0 when the potential scan is reversed at –0.60 V (Figure 2a), but extending the scan to more

(10) Swistak, C.; Mu, X. H.; Kadish, K. M. *Inorg. Chem.* **1987**, *26*, 4360–4366.
(11) Lin, X. Q.; Kadish, K. M. *Anal. Chem.* **1985**, *57*, 1498–1501.
(12) Bottomley, L. A.; Kadish, K. M. *Inorg. Chem.* **1981**, *20*, 1348–1357.
(13) The first electroreduction of [(Tp-$CF_3$PP)Fe]$_2$O occurs at $E_{1/2}$ = –0.94 V in PhCN, 0.1 M TBAP.

**Table I.** Half-Wave Potentials (V vs SCE) of (P)Fe($C_6H_5$) and (P)Fe($C_6F_4X$) (X = H or F) in PhCN, 0.1 M (TBA)$PF_6$

| porphyrin ring, P | axial ligand | σ-bonded complex I | σ-bonded complex II[a] | product IV[b] | product V[d] | product III[e] |
|---|---|---|---|---|---|---|
| OEP | $C_6H_5$ | −0.93 | | | | |
| | $C_6F_5$ | −0.59 | −1.83 | −0.94 | −1.32 | |
| | $C_6F_4H$ | −0.64 | −1.86 | −0.80[c] | −1.34 | |
| TmTP | $C_6H_5$ | −0.72 | | | | |
| | $C_6F_5$ | −0.42 | −1.66 | −0.67[c] | −1.07 | −1.74 |
| | $C_6F_4H$ | −0.46 | −1.64 | −0.71[c] | −1.11 | −1.75 |
| TPP | $C_6H_5$ | −0.70 | | | | |
| | $C_6F_5$ | −0.42 | −1.60 | −0.74 | −1.07 | −1.70 |
| | $C_6F_4H$ | −0.45 | −1.62 | −0.78 | −1.09 | −1.72 |
| Tp-$CF_3$PP | $C_6H_5$ | −0.57 | −1.84 | | | |
| | $C_6F_5$ | −0.34 | −1.48 | −0.61[c] | −0.98 | −1.61 |
| | $C_6F_4H$ | −0.38 | −1.48 | −0.62[c] | −0.98 | −1.60 |

[a] $E_{pc}$ at 0.1 V/s. [b] (P)Fe(OH) + $e^-$ ⇄ (P)Fe + $OH^-$. [c] $E_{pa}$ at 0.1 V/s. [d] $[(P)Fe]_2O + e^- \rightleftarrows [(P)Fe]_2O^-$. [e] $[(P)Fe^I]^- + e^- \rightleftarrows [(P)Fe]^{2-}$.

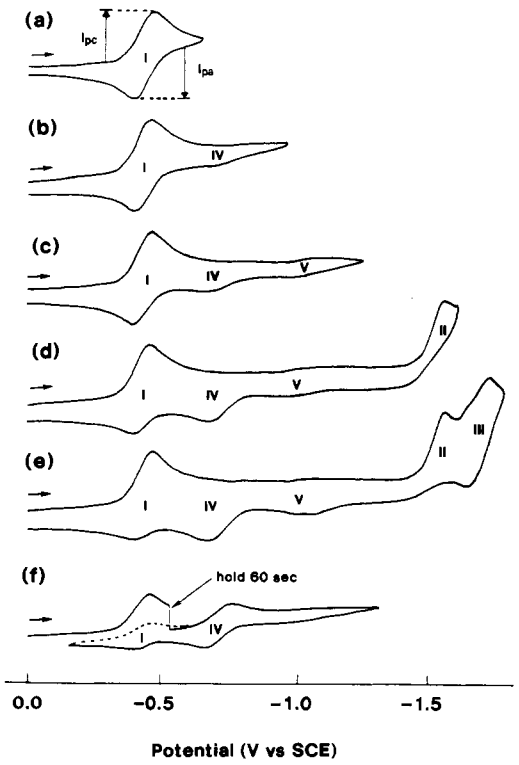


**Figure 2.** Cyclic voltammograms illustrating reduction of (Tp-$CF_3$PP)Fe($C_6F_4H$) at different switching potentials in PhCN containing 0.1 M (TBA)$PF_6$. Scan rate = 0.1 V/s.

negative values results in a decrease of this ratio and the appearance of processes IV and V, both of which have currents smaller than those for the first one-electron reduction (see Figure 2b,c). The value of $i_{pa}/i_{pc}$ is about 0.5 when the scan is reversed at a potential negative of processes II (Figure 2d), and under these conditions a well-defined process IV is observed on the reverse positive sweep. The maximum current for the reoxidation of process IV, $i_{pa}$, increases even further upon scanning beyond reduction process III (Figure 2e), and at the same time the anodic current for process I is decreased even further in magnitude.

Voltammograms were also taken under conditions where the initial negative potential scan was held at −0.50 V for 60 s prior to continuing the sweep to −1.25 V and then reversing the scan direction. An example of the resulting current–voltage curve is shown in Figure 2f, and when combined with the data in Figure 2c–e, indicates that the electroactive species associated with process IV can be generated in either its neutral or singly-reduced form after either the first, the second, or the third electroreduction of (Tp-$CF_3$PP)Fe($C_6F_4H$) in PhCN.

Clear evidence that process IV results from a homogeneous

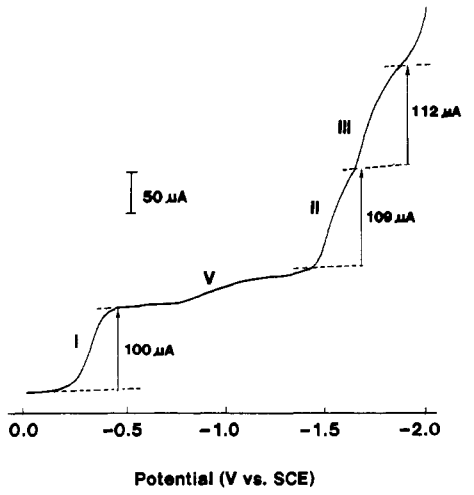


**Figure 3.** Rotating disk voltammogram of (Tp-$CF_3$PP)Fe($C_6F_5$) in PhCN containing 0.1 M (TBA)$PF_6$. Rotation rate = 500 rpm; scan rate = 0.2 V/s.

chemical reaction is given by data for the reduction of (Tp-$CF_3$PP)Fe($C_6F_5$) in PhCN at a rotating disk electrode (RDE). Three major reductions are seen under these conditions (Figure 3). These are labeled processes I–III and have approximately the same $E_{1/2}$ values at the RDE as those measured by cyclic voltammetry. The limiting currents are similar for all three processes, and the overall data are consistent with three one-electron reductions of the initial (Tp-$CF_3$PP)Fe($C_6F_5$) complex. Process IV is not observed, indicating that it is not due to reduction of a species initially present in the bulk of solution. However, this is not the case for reaction V, which is observed and suggests the presence of a second reducible species in solution.

The relative concentrations of the porphyrin species involved in reduction process I and that in process IV were determined by measuring currents for the first two reductions of (Tp-$CF_3$PP)-Fe($C_6F_5$) at different potential scan rates in $CH_2Cl_2$, 0.1 M TBAP and then comparing these values to currents for the two reversible one-electron oxidations of the initial complex under the same experimental conditions (Figure 4a). Both oxidations (processes VI and VII) involve diffusion-controlled one-electron transfers, and the maximum peak current for the first reduction of (Tp-$CF_3$PP)Fe($C_6F_5$) should therefore be equal to that for the first oxidation of the same species in the absence of a coupled chemical reaction; i.e., $i_{pc}(I)/i_{pa}(VI)$ should be equal to unity. This is the case at potential scan rates greater than 20 V/s but not at lower potential scan rates, as shown in Figure 4, which illustrates the cyclic voltammograms obtained at four different potential scan rates and also presents plots of $i_{pc}(I)/i_{pa}(VI)$ and $i_{pa}(IV)/i_{pa}(VI)$ as a function of potential scan rate between 0.02 and 20 V/s. The first peak current ratio depends upon the relative concentration of the species associated with reduction process I, i.e., the concentration of (Tp-$CF_3$PP)Fe($C_6F_5$), while the second is related to the relative concentration of the chemically generated species associated with process IV. As seen in this figure, an increase in the potential scan rate from 0.02 to 20 V/s results in a decrease of $i_{pa}(IV)/i_{pa}(VI)$ and a concomitant increase of $i_{pc}(I)/i_{pa}(VI)$. The currents for process IV are quite small with respect to those for processes VI and VII at a scan rate of 20 V/s, and this contrasts with the data at 0.02 V/s, where process IV is fully developed and process I has almost completely disappeared. These results are consistent with those observed at the rotating disk electrode and give further evidence that process IV is due to a species generated in a chemical reaction following process I. Also, it should be noted that the cathodic peak current of process IV is higher than that of process I but almost identical to that of process VI at a scan rate of 0.02 V/s. This could only occur if the species reduced in process IV were generated by a chain reaction which would decrease the concentration of (Tp-$CF_3$PP)Fe($C_6F_5$) at the

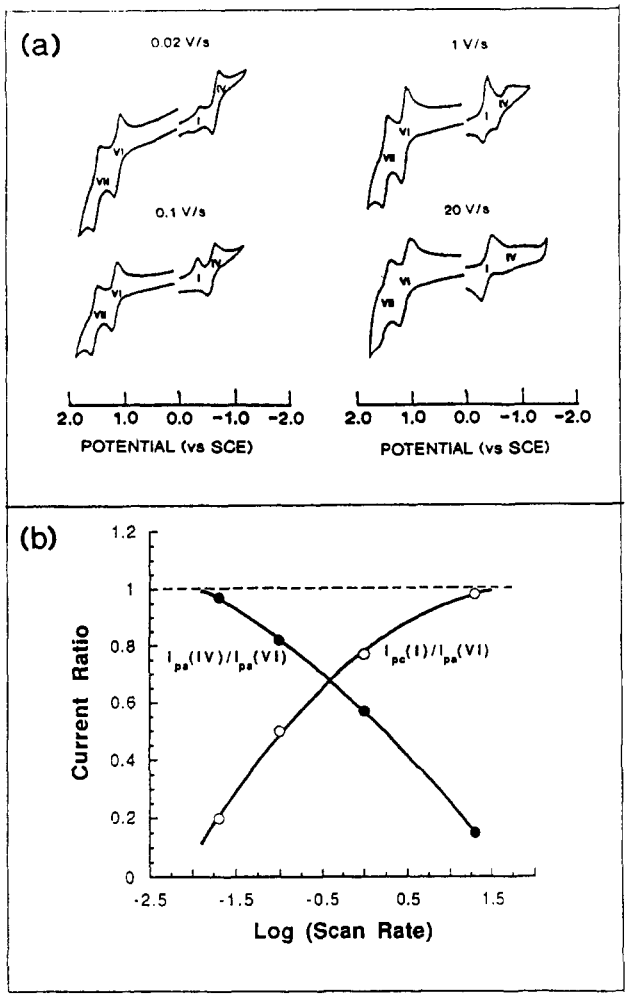


**Figure 4.** (a) Cyclic voltammograms of (Tp-$CF_3$PP)Fe($C_6F_5$) at different scan rates in $CH_2Cl_2$, 0.2 M (TBA)$PF_6$ and (b) relative peak current ratios for processes I and IV with respect to process VI.

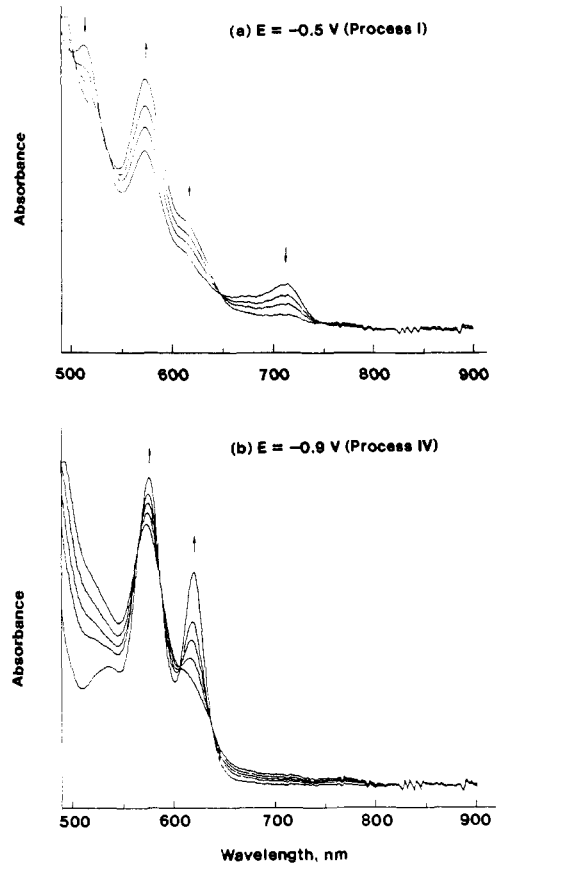


**Figure 5.** UV–visible thin-layer spectral changes of (Tp-$CF_3$PP)Fe($C_6F_5$) in PhCN, 0.2 M (TBA)$PF_6$ during controlled-potential reduction at (a) –0.5 V and (b) –0.9 V.

**Scheme I**

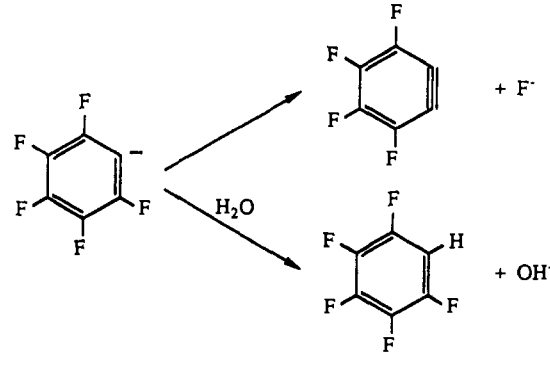


electrode surface prior to its electroreduction. This is the case, as will be demonstrated in following sections of this paper.

**Spectral Characterization of Reduction Products.** The products generated in processes I and IV of (Tp-$CF_3$PP)Fe($C_6F_5$) were investigated by thin-layer UV–visible spectroelectrochemistry, and the resulting data are shown in Figure 5. (Tp-$CF_3$PP)Fe($C_6F_5$) has bands at 523, 572, and 714 nm while the species produced at –0.50 V has a well-defined visible band at 570 nm and a shoulder at 617 nm. Isosbestic points are seen at 534, 648, and 741 nm, but the spectral changes are irreversible and no further changes occur upon switching the potential back to 0.0 V. The final UV–visible spectrum after reduction of (Tp-$CF_3$PP)Fe($C_6F_5$) at –0.50 V is characteristic of a high-spin Fe(III) porphyrin with an anionic axial ligand,[12,14] and an anionic axial ligand also seems to be coordinated to the iron center after further reduction at –0.90 V, i.e., at a potential more negative than that of process IV. These spectral changes are shown in Figure 5b. The UV–visible spectrum after complete electrolysis at this potential has bands at 574 and 614 nm and has the characteristic spectral pattern of a $[(P)Fe^{III}X]^-$ derivative where X is an anionic axial ligand.[15]

The initial reduction of (Tp-$CF_3$PP)Fe($C_6F_5$) should lead to an Fe(II) complex but the spectroscopic results suggest that the ultimate porphyrin product generated in a thin layer cell at –0.50 V contains high-spin Fe(III).[12] One must therefore consider the possibility of reduction at a site other than the metal center or, alternatively, the possibility that an Fe(III) porphyrin complex other than the original $\sigma$-bonded one is regenerated *via* a homogeneous chemical reaction following process I.

A direct electroreduction of the $C_6F_4X$ axial ligand or the porphyrin macrocycle is highly unlikely. The electrochemical behavior of (P)Fe($C_6F_4X$) differs from that of all previously studied iron porphyrins and this could suggest that the bound or axially dissociated fluorophenyl axial ligand is directly involved in a chemical reaction. Two competing reactions of liberated $C_6F_4X^-$ (X = H or F) are possible.[16] The first involves a loss of $F^-$ to give fluorobenzyne derivatives while the second involves a reaction with a water molecule from the solvent to give $C_6F_4XH$ and $OH^-$, as shown in Scheme I for the case of a $C_6F_5^-$ ligand.

Both fluoride and hydroxide anions will strongly complex to iron(II) and iron(III) porphyrins,[15,17-23] and this will first produce

(14) Kadish, K. M. In *Iron Porphyrins*; Lever, A. B. P., Gray, H. B., Eds.; Addison-Wesley: Reading, MA, 1983; Vol. II, Part 2, Chapter 4, pp 161–249.
(15) Kadish, K. M.; Rhodes, R. K. *Inorg. Chem.* **1983**, *22*, 1090–1094.
(16) Callander, D. D.; Coe, P. L.; Tatlow, J. C. *Tetrahedron* **1966**, *22*, 419–432.
(17) Tung, H. C.; Chooto, P.; Sawyer, D. T. *Langmuir* **1991**, *7*, 1635–1641.

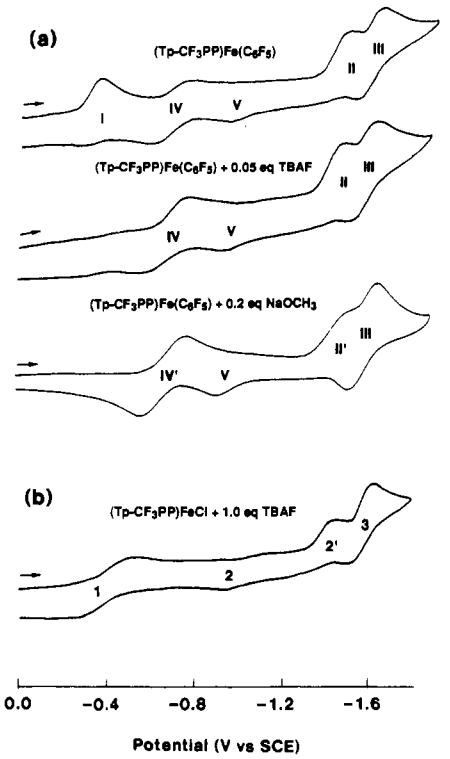


**Figure 6.** Cyclic voltammograms of (a) (Tp-$CF_3$PP)Fe($C_6F_5$), (Tp-$CF_3$PP)Fe($C_6F_5$) + 0.05 equiv of (TBA)F, and (Tp-$CF_3$PP)Fe($C_6F_5$) + 0.2 equiv of $NaOCH_3$ and (b) (Tp-$CF_3$PP)FeCl + 1.0 equiv of (TBA)F in PhCN containing 0.2 M (TBA)$PF_6$.

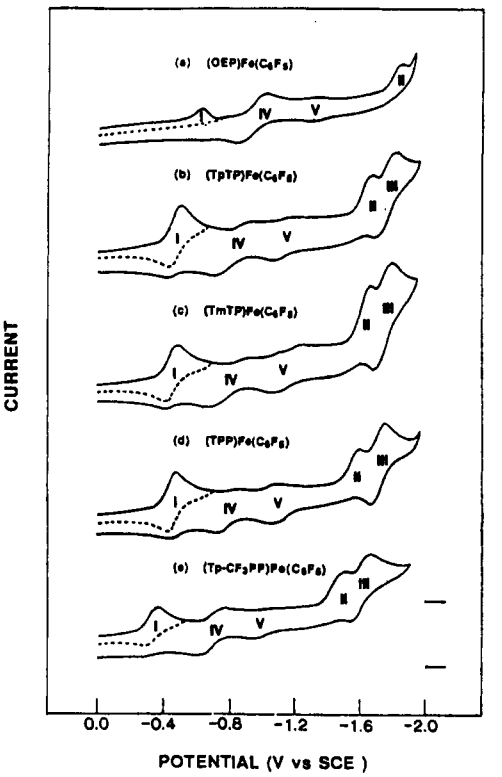


**Figure 7.** Cyclic voltammograms of (a) (OEP)Fe($C_6F_5$), (b) (TpTP)Fe($C_6F_5$), (c) (TmTP)Fe($C_6F_5$), (d) (TPP)Fe($C_6F_5$), and (e) (Tp-$CF_3$PP)Fe($C_6F_5$) in PhCN containing 0.1 M (TBA)$PF_6$. Scan rate = 0.1 V/s.

(P)$Fe^{III}F$, (P)$Fe^{III}OH$, [(P)$Fe^{II}F$]$^-$, or [(P)$Fe^{II}OH$]$^-$, depending upon the metal oxidation state. The two hydroxide complexes, (P)$Fe^{III}OH$ and [(P)$Fe^{II}OH$]$^-$, can also be converted to a μ-oxo dimer on longer time scales, and this species must also be considered as a possible ultimate reduction product of electrode process I.

The spectral data in Figure 5a,b are most consistent with $F^-$ or $OH^-$ type derivatives, but a differentiation between these two derivatives is not possible from the UV–visible spectra alone. However, iron porphyrins containing $OH^-$ and $F^-$ axial ligands differ in their electrochemistry,[4,10,12,17-23] and this fact was therefore utilized to determine which porphyrin products are most likely present in solution after process I under the given experimental conditions.

Cyclic voltammograms obtained upon addition of (TBA)F or $NaOCH_3$ to (Tp-$CF_3$PP)Fe($C_6F_5$) in PhCN are illustrated in Figure 6a. Nonsterically hindered iron porphyrins are known to dimerize in the presence of $OH^-$ but not $OCH_3^-$. The electrochemistry of iron porphyrins containing $OH^-$ and $OCH_3^-$ axial ligands is similar,[10] and the electrochemical behavior of (Tp-$CF_3$PP)Fe($C_6F_5$) was therefore investigated in the presence of $OCH_3^-$ rather than $OH^-$ in order to avoid dimerization. The cyclic voltammograms of (Tp-$CF_3$PP)Fe($C_6F_5$) in the presence of (TBA)F and $NaOCH_3$ are virtually identical, and both differ from that of (Tp-$CF_3$PP)Fe($C_6F_5$) in the absence of added ligands in that they show no evidence for process I. Similar redox processes are observed in all three voltammograms, and these occur at almost the same potentials under all three experimental conditions. The key point in Figure 6a is that only 0.05 equiv of (TBA)F is needed to cause the complete loss of process I and the full development of process IV. The addition of 0.2 equiv of $NaOCH_3$ to PhCN solutions of (Tp-$CF_3$PP)Fe($C_6F_5$) also produces the same result, and these data are thus both consistent with a chain reaction which facilitates removal of the σ-bonded axial ligand from (Tp-$CF_3$PP)Fe($C_6F_5$) prior to electroreduction.

The identity of the anion produced ($OH^-$ or $F^-$) from $C_6F_5^-$ (Scheme I) was further elucidated by examining the electrochemistry of a genuine (Tp-$CF_3$PP)FeF complex in PhCN and comparing the potentials for reduction of this porphyrin to the $E_{1/2}$ values for processes II–V of (Tp-$CF_3$PP)Fe($C_6F_4X$). The five-coordinate (Tp-$CF_3$PP)FeF complex was obtained by adding 1.0 equiv of (TBA)F to (Tp-$CF_3$PP)FeCl and gave the cyclic voltammogram shown in Figure 6b. Three reductions are observed. Processes 2 and 2′ are coupled to each other.

The first reduction of (Tp-$CF_3$PP)FeF is located at $E_{1/2}$ = –0.42 V, which differs substantially from the $E_{1/2}$ of –0.98 V for process IV. This difference in reduction potentials clearly rules out formation of a five-coordinate $F^-$ complex as the porphyrin species generated after process I. (Tp-$CF_3$PP)FeOH is therefore the most likely Fe(III) reduction product since $E_{1/2}$ of process IV is virtually identical to $E_{1/2}$ for reduction of homogeneously generated (Tp-$CF_3$PP)Fe$OCH_3$ in PhCN (Figure 6a).

**Effect of Porphyrin Macrocycle on Electrochemistry.** The electrochemical behavior of four additional fluorophenyl σ-bonded iron(III) porphyrins was also investigated, and cyclic voltammograms of all five compounds are illustrated in Figure 7. The first reduction is reversible for four of the compounds at a scan rate greater than 0.1 V/s, but this is not the case for (OEP)Fe($C_6F_5$), which is irreversibly reduced (see dashed lines in Figure 7). This result suggests that the stability of the product electrochemically generated in process I is decreased for porphyrins having a higher ring basicity such as in the case of OEP. Process II is irreversible for all five investigated porphyrins while process III is reversible. $E_{1/2}$ for this latter reduction is close to $E_{1/2}$ for the third electroreduction of (P)FeCl derivatives having

(18) Srivasta, G. S.; Sawyer, D. T. *Inorg. Chem.* **1985**, *24*, 1732–1734.
(19) Sawyer, D. T. *Comments Inorg. Chem.* **1990**, *10*, 129–159.
(20) Lexa, D.; Momenteau, M.; Saveant, J. M.; Xu, F. *Inorg. Chem.* **1985**, *24*, 122–127.
(21) Cohen, I. A.; Lavallee, D. K.; Koplove, A. B. *Inorg. Chem.* **1980**, *19*, 1098–1100.
(22) Gans, P.; Marchon, J.-C.; Moulis, J. M. *Polyhedron* **1982**, *11*, 737–738.
(23) Phillippi, M. A.; Shimomura, E. T.; Goff, H. M. *Inorg. Chem.* **1981**, *20*, 1322–1325.

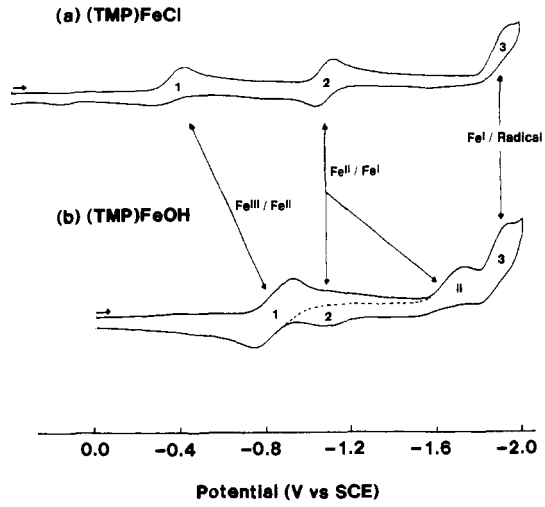


**Figure 8.** Cyclic voltammograms of (a) (TMP)FeCl and (b) (TMP)FeOH at a scan rate of 0.1 V/s in PhCN, 0.1 M (TBA)P.

the same porphyrin macrocycle,[4,14] and this suggests that process III involves the same reacting species.

In summary, the data in Figures 6 and 7 are consistent with the formation of a five-coordinate (P)FeOH species being reduced in process IV and a four-coordinate $[(P)Fe^{I}]^-$ species being reduced in process III. Thus there remains only an identification of those species involved in processes V and II. It was earlier pointed out that $E_{1/2}$ for process V may or may not vary from $E_{1/2}$ of the $(P)Fe^{II}/[(P)Fe^{I}]^-$ reaction, but both of these values are close to $E_{1/2}$ for the first reduction of a $\mu$-oxo dimer having the same porphyrin macrocycle. For example, process V of (OEP)Fe($C_6F_5$) occurs at $E_{1/2}$ = −1.35 V in benzonitrile, 0.1 M TBAP, and this may be compared to an $E_{1/2}$ of −1.37 V for reduction of a genuine $[(OEP)Fe]_2O$ sample under the same solution conditions. In a similar manner, process V of (TPP)Fe($C_6F_5$) occurs at $E_{1/2}$ = −1.10 V, and this can be compared to an $E_{1/2}$ of −1.10 V for reduction of a genuine $[(TPP)Fe]_2O$ sample in PhCN, 0.1 M TBAP.

Electroreduced iron porphyrin dimers are relatively unstable, and none has been characterized as showing a reversible second reduction.[4,17-25] However, an irreversible second reduction of $[(TPP)Fe]_2O$ has been reported to occur at $E_p$ = −1.61 V in $CH_2Cl_2$,[14] and this value is similar to the potential for process II of (TPP)Fe($C_6F_4X$) (see Table I). This electrode reaction can therefore be assigned either as the second reduction of a (TPP)FeOH "decomposition" product or alternatively as the second reduction of homogeneously generated $[(TPP)Fe]_2O$. The most definitive evidence for assignment of process II as a reduction of $[(P)FeOH]^-$ comes from comparisons between the electrochemical behaviors of (TMP)FeCl and (TMP)FeOH, porphyrins which do not dimerize due to steric hindrance of the macrocycle.

Cyclic voltammograms of the two TMP complexes are shown in Figure 8. The main difference between the two voltammograms is the 530-mV shift in the first reduction potential of (TMP)FeOH as compared to (TMP)FeCl and the presence of an irreversible peak at $E_p$ = −1.72 V for the $OH^-$ derivative. This irreversible reduction is labeled as process II in Figure 8 and can only be assigned to the reduction of $[(TMP)FeOH]^-$, since dimeric $[(TMP)Fe]_2O$ cannot be formed and no $Fe^{II}/Fe^{I}$ process is observed in the expected range of potential as seen for (TMP)FeCl.

**Mechanism.** An overall self-consistent mechanism for the reduction of (P)Fe(R) is given in Scheme II where R = $C_6F_5$ or $C_6F_4H$ and the numbers below the electrode processes refer to the peaks in Figures 1–7.

**Scheme II**

**A. Initial Reduction**

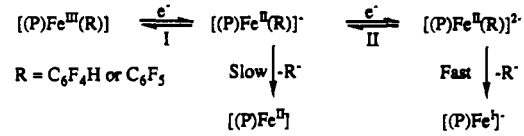


**B. Chemical Chain Reaction**

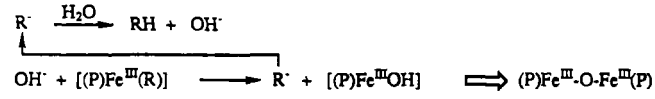


**C. Electrochemistry of Products**

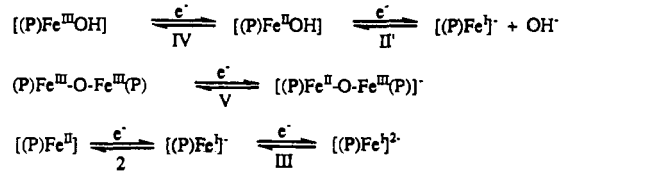


The overall reduction of the initial $(P)Fe^{III}(R)$ complex can be described as occurring in three discrete steps. The first involves the formation of $[(P)Fe^{II}(R)]^-$ and $[(P)Fe^{II}(R)]^{2-}$ (step A), and this is followed by a loss of the $R^-$ group, which participates in a chemical chain reaction (step B) to generate two new iron(III) porphyrins, both of which can be further reduced along with the products of the initial (P)Fe(R) reduction (step C). A total of seven different redox couples can be obtained for a given (P)Fe(R) complex, and three of these (I, IV, and III) occur at discrete well-defined potentials which can be unambiguously assigned to a single characterizable redox process. The other four couples can be divided into two different sets of processes, each of which overlaps in half-wave potentials. These are processes 2 and V, which correspond to the one-electron reduction of $(P)Fe^{II}$ and $[(P)Fe]_2O$,[25] and processes II and II', the first of which corresponds to the reduction of $[(P)Fe^{II}(R)]^-$ while the second corresponds to the reduction of the $[(P)Fe^{II}OH]^-$. The similarity in $E_{1/2}$ values for processes II and II' is not unexpected since both reacting species are five-coordinate Fe(II) porphyrins which possess a single anionic axial ligand.

The key point in the above mechanism is the chemical chain reaction, which involves a conversion of liberated $C_6F_4X^-$ to $C_6F_4XH$ and free $OH^-$, as shown in Scheme I. The hydroxide anion is a stronger axial ligand than $C_6F_4X^-$,[26] and it will therefore displace the $\sigma$-bonded fluorophenyl ligand from $(P)Fe^{III}(R)$ to give $(P)Fe^{III}OH$ in solution. The liberated $R^-$ can then react with an additional water molecule to generate another $OH^-$ anion, which will further react with (P)Fe(R) to give more (P)FeOH and another $R^-$ molecule, as shown in step B of Scheme II. The relative rate of this chain reaction with respect to the potential scan rate will determine the relative heights for reduction processes I and IV (see Figure 2), with the limiting factor being the concentration of water in solution. The addition of substoichiometric amounts of $F^-$ or $OCH_3^-$ to solutions of (P)Fe($C_6F_4X$) can also initiate the chain reaction (see Figure 6), which will then continue to propagate until completion. This occurs when the $C_6F_4X^-$ group is initially liberated in a straightforward ligand exchange involving the added anion and the axially coordinated ligand $C_6F_5^-$ or $C_6F_4H^-$.

(24) Stolzenberg, A. M.; Strauss, S. H.; Holm, R. H. *J. Am. Chem. Soc.* **1981**, *103*, 4763–4778.
(25) Kadish, K. M.; Larson, G.; Lexa, D.; Momenteau, M. *J. Am. Chem. Soc.* **1975**, *97*, 282–288.
(26) The first one-electron reduction of (P)FeOH is cathodically shifted by greater than 400 mV compared to reduction of the analogous (P)Fe($C_6F_4X$) complex in a noncoordinating solvent.

Further electrochemical evidence for the occurrence of a chain reaction follows from bulk-controlled potential coulometry of (Tp-$CF_3$PP)Fe($C_6F_5$) in PhCN. A bulk electrolysis of (Tp-$CF_3$PP)Fe($C_6F_5$) at –0.50 V consumes less than 0.1 electron, and this contrasts with the expected $n$ = 1.00 if process I involved only a simple electron transfer or an electron transfer which was followed by a chemical reaction which did not involve a chain reaction. The first reduction of (Tp-$CF_3$PP)Fe($C_6F_5$) is irreversible, and no electrons are transferred when the bulk-reduced solution is reoxidized at 0.00 V. As expected, the cyclic voltammogram obtained after bulk reduction at –0.5 V shows no evidence of process I, indicating a complete conversion of the initial (Tp-$CF_3$PP)Fe($C_6F_5$) complex to (Tp-$CF_3$PP)FeOH and/or [(Tp-$CF_3$PP)Fe]$_2$O. Further electrolysis of the chemical product at –0.9 V (process IV) consumes about 0.5 electron, and another 0.5 electron is consumed at –1.2 V (process V), yielding a total of about one electron added for the combined processes IV (the $OH^-$ derivative), V (the μ-oxo dimer), and 2 (which corresponds to the reaction of (P)$Fe^{II}$).

**Summary.** The mechanism described in the present paper for the reduction of (P)Fe($C_6F_5$) and (P)Fe($C_6F_4H$) differs from that of all previously investigated iron porphyrins, and this is due entirely to the presence of the σ-bonded fluorophenyl ligand. The first reduction of (P)Fe(R) leads to (P)$Fe^{II}$ and $R^-$, the latter of which reacts with trace water in solution to give $OH^-$ and RH. The generated $OH^-$ displaces the axial fluorophenyl ligand from unreduced (P)Fe(R), and this sets in motion a chain reaction which continues until all of the σ-bonded porphyrin is converted to monomeric (P)FeOH prior to formation of dimeric [(P)Fe]$_2$O on longer time scales. The same Fe(III) porphyrin products can also be obtained by addition of substoichiometric amounts of $F^-$ or $OCH_3^-$ to (P)Fe(R), and this occurs because both anions are able to displace the fluorophenyl axial ligand from (P)Fe(R) and initiate the chain reaction in the absence of any electrochemistry.

All of the studies described above were carried out in rigorously dry solvents whose water content was estimated to be <0.005%. This amount of water is sufficiently low so that any $OH^-$ produced upon dissociation would be totally negligible with respect to the porphyrin, whose concentration ranges from $10^{-4}$ to $10^{-3}$ M for electrochemistry and from $10^{-5}$ to $10^{-4}$ M for UV–visible spectroscopy. On the other hand, equimolar concentrations of $OH^-$ and porphyrin are produced upon the reaction of $R^-$ with water. Even under the best conditions, most anhydrous solvents will contain at least $3 \times 10^{-4}$ M water, and this can be quantitatively converted to the same concentration of $OH^-$ at potentials sufficiently negative to initiate the reduction of (P)Fe(R). Finally, it should be pointed out that a complexation of the reduced or neutral porphyrin by $OH^-$ can be prevented by carrying out electrochemistry of the σ-bonded complex in the presence of a stronger axial ligand, especially one which is present in higher concentration than that of the metalloporphyrin or $OH^-$. This is exactly what is seen in pyridine[3] and explains the higher stability of the neutral and singly-reduced hexacoordinated (P)Fe(R)(py) species in this solvent.

**Acknowledgment.** The support of the CNRS, the National Institutes of Health (K.M.K.; Grant GM 25172), the National Science Foundation (K.M.K.; Grant CHE-90-01381), and NATO (Grant 0168(87)) is gratefully acknowledged. The help of C. Ratti, Y. H. Liu, and L. Courthaudon in preliminary experiments is also gratefully acknowledged.